JCEC
THE JOURNAL OF ENGINEERING AND EXACT SCIENCES

OPEN ACCESS

The Journal of Engineering and Exact Sciences – jCEC, Vol. 10 N. 09 (2024)
journal homepage: https://periodicos.ufv.br/jcec
eISSN: 2527-1075
ISSN: 2446-9416

Rheological analysis of cemented carbides and Tungsten powders for additive manufacture via laser powder bed fusion technique

Análise reológica de carbonetos cementados e pós de tungstênio para manufatura aditiva por meio da técnica de fusão a laser em leito de pó

Article Info:
Article history: Received 2024-11-05 / Accepted 2024-12-12 / Available online 2024-12-15
doi: 10.18540/jcecvl10iss9pp20994

Fábio Miranda
ORCID: https://orcid.org/0000-0003-2867-1028
Escola Politécnica USP & BRATS Indústria e Com. de Produtos Metálicos Especiais Ltda, Brazil
E-mail: fabio.miranda@usp.br
Rodrigo Condotta
ORCID: https://orcid.org/0000-0001-6524-1233
Centro Universitário FEI, Brasil
E-mail: rcondotta@fei.edu.br
Nathalia Marina Gonçalves Pereira
ORCID: https://orcid.org/0009-0007-9314-3156
Centro Universitário FEI, Brasil
E-mail: unienpereira@fei.edu.br
Marcelo Otávio dos Santos
ORCID: https://orcid.org/0000-0002-2357-6593
Escola Politécnica USP & Instituo Mauá de Tecnologia, Brazil
E-mail: marcelo.santos@maua.br
Daniel Rodrigues
ORCID: https://orcid.org/0000-0003-4327-5162
BRATS Indústria e Comércio de Produtos Metálicos Especiais Ltda, Brazil
E-mail: daniel@brats.com.br
Suzilene Real Janasi
ORCID: https://orcid.org/0000-0001-7984-5994
BRATS Indústria e Comércio de Produtos Metálicos Especiais Ltda, Brazil
E-mail: srjanasi@yahoo.com.br
Fernando dos Santos Ortega
ORCID: https://orcid.org/0000-0001-5915-2453
Univ. do Vale do Paraíba & BRATS Ind. e Com. de Produtos Metálicos Especiais Ltda, Brazil
E-mail: ortega@univap.br
Gilmar Ferreira Batalha
ORCID: https://orcid.org/0000-0001-8625-8499
Escola Politécnica USP & BRATS, Brazil
E-mail: gfbatalh@usp.br

Abstract
In Additive Manufacturing (AM) using the Laser Powder Bed Fusion (L-PBF) technique, spherical powders are the most commonly preferred for direct sintering. However, composites such as cemented carbides and heavy alloys often exhibit irregular shapes. Due to the requirement for extremely fine grain size, the cohesive behavior of the particle bed becomes significant, influencing its compressibility and porosity. These physical properties result in powders with coarse textures,

which lead to low fluidity and interruptions in material flow within the ducts. This study evaluates the flowability of WC and W refractory materials combined with Co and Ni. Key interparticle properties, including real and bulk density, bulk compressibility and porosity, and granular shear, were analyzed to understand their influence on the deposition layer behavior in the powder bed. These parameters are crucial for understanding the micro-behavior of granular materials and correlating it with their macro-behavior. The rheological aspects of these composite powders are discussed, aiming to establish correlations between the manufacturing process and the resulting properties of their mixtures.
Keywords: Rheological behavior of powder composites. Flowability of heavy alloys. Properties and applications of powder bed fusion. Behavior of cermets in additive manufacturing.

1. Introduction

The qualities of the parts manufactured by Additive Manufacturing (AM) are influenced by the characteristics of the powders, such as size distribution, surface morphology, composition, and flowability of the particulates (Debroy *et al.*, 2018). Typical particle sizes for sintering via L-PBF range from 10 to 60 µm. The behavior of a composite or ceramic powder is crucial to its performance in the manufacturing process, particularly during compaction, where the filling of molds or die powder spreading depends on flowability. Various methods and tests can help evaluate dynamic flow and flowability, but determining the optimal flow conditions is not always straightforward. (Marchetti *et al.*, 2021).

In the AM technique, experimental characterization of powders typically includes average diameter, particle size distribution, and bulk density, which are not enough to solve a specific configuration for powder bed deposition (Debroy *et al.*, 2018; Marchetti *et al.*, 2021).

Powdered composites used in additive manufacturing are spread onto a compacted layer for direct sintering, with the process repeated layer by layer to build the product. Various measurement techniques are available to evaluate the flowability of these powders. They can be divided into categories (Miranda *et al.*, 2023a), such as flow rate, density rates, bulk and tapped densities angle of repose, and frictional forces, among other methods (Debroy *et al.*, 2018; Marchetti *et al.*, 2021; Miranda *et al.*, 2023a; 2023b; 2024). The differences between these methods can be significant, as each test method influences the stress state, particle velocity, bulk density, tapped density, and other factors that affect the feed flow behavior (Debroy *et al.*, 2018; Marchetti *et al.*, 2021). In general, the physical properties of pure powders or composites have a direct influence on the manufacturing process parameters via L-PBF. The main properties are the shapes of the particles, the size distribution of the grains, and the apparent density, which determine the thickness of the deposited layers in the bed (Pal *et al.*, 2018).

The packing of powders can be quantified based on their bulk/tapped densities ratio. Flowability tests allow us to obtain the mass flow rate and the bulk density (Miranda *et al.*, 2023a; 2023b; 2024). However, it is known that the quality of the dry granulate significantly impacts the compaction processes, which are influenced by the rheological properties of the granulates. On the other hand, it has been found in other studies that powders with the same particle size can flow differently due to the effects of other properties, such as texture, surface shape, and agglomeration (Freeman *et al.*, 2016).

This study is part of an ongoing project and will highlight how the parameters of powder composites influence the final density of the product in the powder bed for the AM L-PBF technique. A vibrating container-type device was developed, coupled with a metallic roller (Figure 1), whose rotation speed is controlled independently of its displacement speed. Compaction is done with a polished stainless steel metal roller inside the sintering chamber in the powder bed (Figure 1). Compacting thin layers with a compactor roller is important for extra-fine powder composites in three-dimensional printing techniques (Budding & Vaneker, 2013). In this roller compactor operation, the powdered composites need to flow beneath the fluidizing container and, at the same time, are spread and compacted.

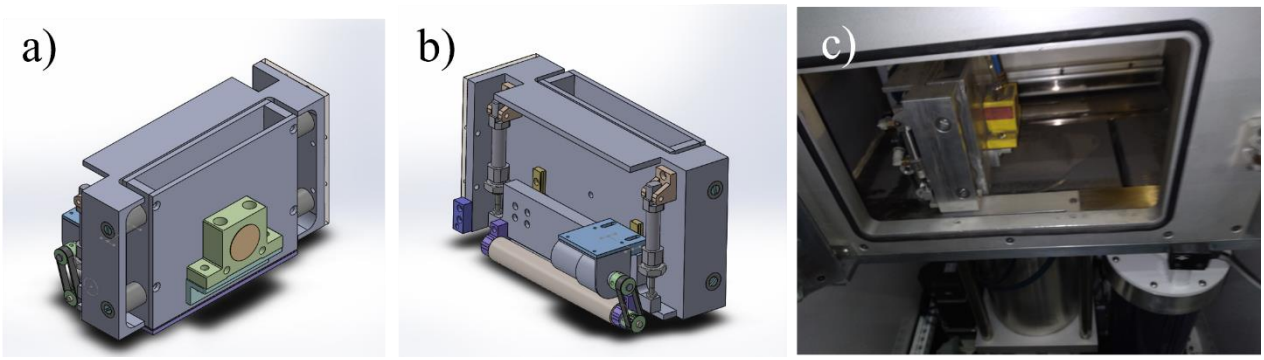

Figure 1 – Isometric perspectives of the powder container and vibrating device coupled with a compactor roller, (A) Front View and (B) Back View, and (C) sintering chamber and vibrating device installed inside the sintering chamber.

To achieve this, it was necessary to select and determine an appropriate sieve or stainless-steel mesh to control the deposition flow of powders from the prepared mixtures. The powder bed layer is created using a vibrating device (capacity 1,500 g) equipped with a rubber scraper and a compactor roller at the bottom (Figure 1-B). The speed of the device and the rotation of the roller are controlled. The powder bed area is vast (about 630 cm^2), and the compaction force is applied by a 2.0 kg (19.613 N) roller. The powder drains from the device through a #35 mesh/Tyler sieve (Miranda *et al.*, 2023a). The translational movement of the device simultaneously spreads and compacts the powder, generating layers in the powder bed of 30 to 100 µm. As depicted in Figure 1-C, the sintering chamber is purged with a continuously flowing, high-purity argon atmosphere at a rate of 0.3 L/min. Several operational parameters associated with this new compaction strategy can be adjusted and controlled to modify the compacted layer in the dust bed; the effect of roller compaction force on the properties of powdered composites is one of the main variables. The rheological properties of the granules are influenced by the processing parameters: compressibility, bulk/tapped density, aeration, the basic energy of flow, and shear (Costa, Costa & Condotta, 2015; Freeman *et al.*, 2016; Gururajan *et al.*, 2005). Nevertheless, it is quite challenging to observe the powder spreading and compaction processes in order to obtain critical parameters that directly demonstrate their influence on the performance of the compacted layer in the powder bed (Miranda *et al.*, 2023a; 2023b; 2024). For this device, Figure 1-C, it is not possible to assess the rheological behavior of the powder composites to determine the flow energy of the samples and quantify the flow resistance of the mixtures in the process of creating the powder bed. In this context, a FT-4 Powder Rheometer® (Freeman Technology) was used to analyze the rheological behavior of certain composite powders used in L-PBF, measuring dynamic flow, compressibility, aeration, and shear behavior.

2. Experimental

Samples of powdered composites of WC and W-based alloys were prepared using the raw materials listed in Table I, with the compositions presented in Table II, according to the methodology described in previous scientific works (Miranda *et al.*, 2023a; 2023b; 2024). High-purity commercial WC, W, Co and Ni powders were used, and their visual characteristic is exhibited in Figure 2. All sample powder were subjected to particle size distribution analysis using the laser diffraction technique (Microtrac S 3500) in aqueous media after 3 minutes of ultrasonication.. The real particle density values obtained by helium pycnometer (AccuPyc II 1350) and BET specific surface area was measured by N_2 physisorption (Gemini II) of the raw materials. The full experimental protocol for these measurements is described in a previous work (Miranda *et al.*, 2023a),

The composites were prepared by mixing pure components in a high shear rate mixer for 2 hours. Isopropyl alcohol was added to the powders to ensure a homogeneous suspension, preventing deformation and breakage of the particulates. Next, the suspension was dried in an oven at 200°C

for 2 hours to remove the isopropyl alcohol.The powder mixtures were than deagglomerated and classified in a sieve series, according to NBR-5734. These mixing and deagglomeration processes are usually employed to prepare powder mixtures for the L-PBF process.

Table I - Properties of refractory ceramic and metallic powders (Miranda *et al.*, 2023b; 2024).

Powders	Density (g.cm^{-3})		Grain Size	Purity	Origin
	Theoretical	Apparent	(μm)	(%)	(manufacturer)
WC	15.63	4.0	1.5	99.53	Buffalo Tungsten Inc.
W	19.25	5.6	1.5	99.76	Buffalo Tungsten Inc.
Co	8.90	2.0	2.0	99.97	Nanjing Henri Cobalt
Ni	8.91	2.5	4.8	99.85	CVMR Corporation

Compared to Nickel, pure Co powder is constituted by large irregular agglomerates of spherical particles. Moreover, its interstitial void is easily observed, which may contribute to the lower bulk density of this specimen. Although agglomerates nickel powder also presents agglomerates, it is more uniform in terms of particle size and shape, with reduced visible interstitial voids.

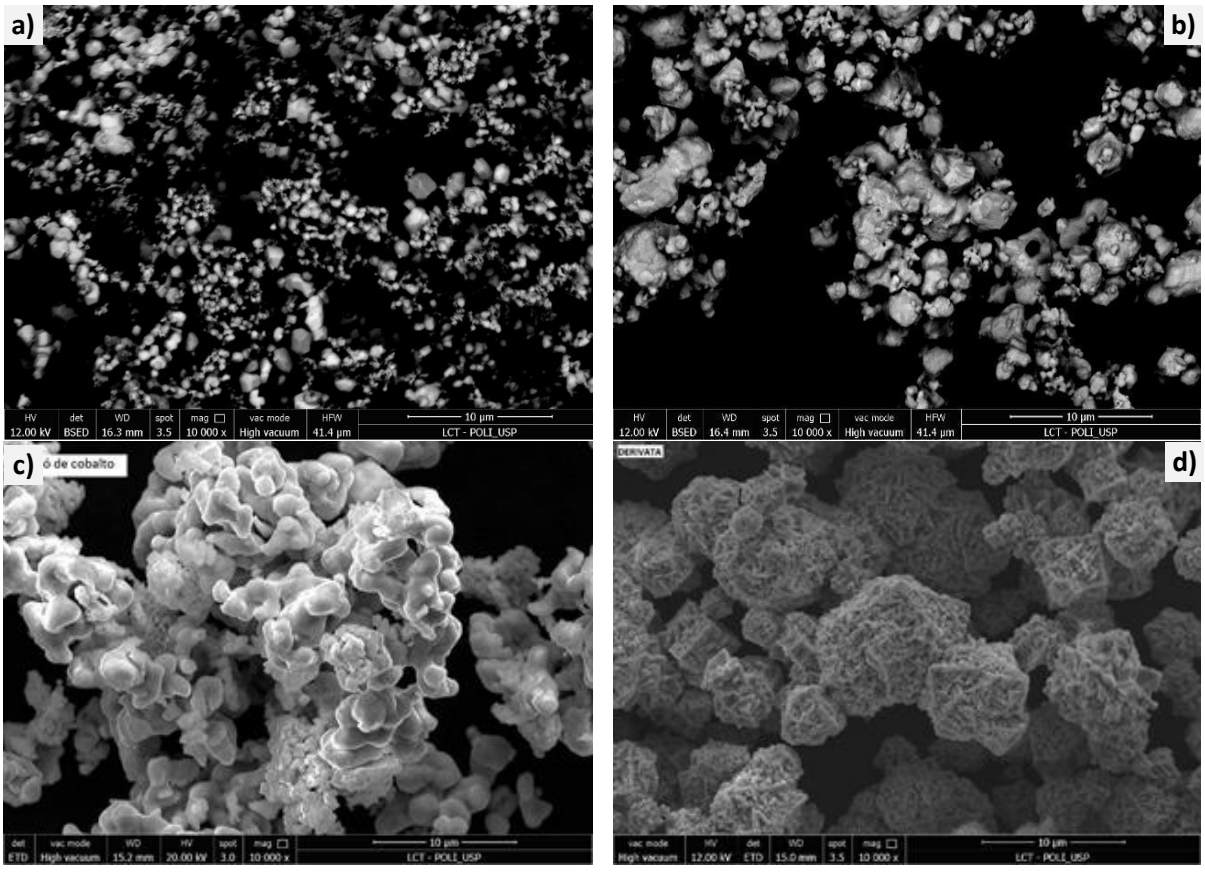

Figure 2 – Scanning Electron Microscopy (SEM) images obtained by backscattered electron (BEI) of the powders used to prepare the mixtures: a) W; b) WC; c) Co; d) Ni.

Table II - Weight balance of alloys prepared based on WC and W.

Sample #	Sample Name	Balance by weight (%)		
		WC or W	Co	Ni
(I)	70WC-30Co	70.0	30.0	0.0
(II)	70WC-30Ni	70.0	0.0	30.0
(III)	70WC-30(Co,Ni)	70.0	15.0	15.0
(IV)	70W-30Ni	70.0	0.0	30.0

The rheological behavior of these composites was evaluated through standard measurements using an FT-4 Powder Rheometer®. Hence, the basic flow energy (BFE), stability, and variable flow rate (VRF) tests were carried out, which involved measuring the resistance to the passage of a patented twisted blade through the particle bed under a constant blade tip speed of 100 mm/s (for a 48 mm blade diameter). The required force and torque are converted into the flow energy (Freeman, 2007).

Sample stability was also evaluated by repeating the BFE measurements 7 times, as the movement of the blade through the particle bed can alter the packing, promote changes in the interparticle interactions, or even cause surface modifications such as abrasion, breakage, segregation, etc.

Finally, an accurate value of the basic flow energy (BFE) is recorded by the equipment as the average of the measured energy in the 6th and 7th tests after the samples have stabilized.

3. Results and Discussion

The particle size distribution of powdered composites is essential in the production process of sintered parts, as it is intrinsically linked to density and linearity/volumetric shrinkage. Figure 3-a shows the particle size distribution of the raw materials, and it can be noticed that Co powder presents a narrow distribution and an average particle size smaller than 0.1 µm. In contrast, larger particles and a wider size distribution of WC and the other metallic powders are noticed (Ni and Co). These results agree with the MEV-BEI images in Figure 2.

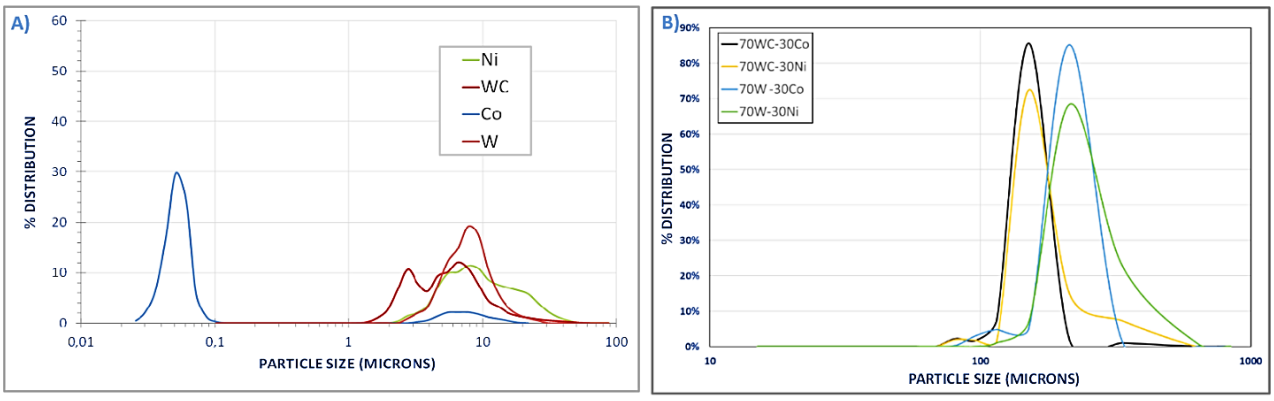

Figure 3 – a) Particle size distribution measured by laser diffraction of the powders used to prepare the mixtures; b) particle size distribution obtained by sieving of 200 grams of powder mixtures after deagglomeration.

The statistical distribution of particle sizes obtained by the sieving measurement process is shown in Figure 3-b. The granules average size was above 100 µm for all powder mixtures, and those containing W presented an average size (280 µm) slightly larger than those containing WC (140 µm). According to the Tyler system, these solid particulates are classified as ultrafine (from 50 to 400 mesh / 38 to 300 µm).

The real density of particles, specific surface area, porosity, and average pore size of the powders are presented in Table III. The values obtained experimentally were compatible with those described in their respective technical data sheets of origin. Cobalt powder presented the highest specific surface area, which is coherent with its particle size and visual morphology observed in Figure 2-C.

Table III - Weight balance of alloys prepared based on WC and W.

Powders	Average particle density ($g.cm^{-3}$)	Surface Area BET ($m^2.g^{-1}$)	Total pores per volume ($cm^3.g^{-1}$)	Average pore diameter (nm)
WC	15.494 ± 0.040	0.624	0.006	35.770
W	N.A.	N.A.	N.A.	N.A.
Co	8.422 ± 0.068	4.667	0.015	13.126
Ni	8.952 ± 0.031	1.252	0.012	38.974

Figures 4-A to 4-D show the MEV- BEI images (backscattered electrons). For the 70WC-30Ni mixture (Figure 4-C), the identification of Ni and Co are the darker particles; what differentiates is the shape of the particles. Ni has a dendritic format, while WC has lighter particles (density 15.494 g.cm-3). These BEI images of the mixtures show the mass balance contrast of the 70WC-30Co, 70WC-30Ni, and 70WC-30(Co, Ni) alloys, respectively. When comparing the same image, the BEI identifies light particles (higher apparent density) from darker particles (lower density).

However, Co and Ni, for the alloy 70W-30(Co, Ni) (Figure 4-D), did not demonstrate this light-dark contrast very well due to the densities of Co (8.422 g.cm-3) and Ni (8.952 g.cm-3) are very close, for better differentiation, through the shapes of the particles it was possible to identify the constituents. Powder composites have irregular particle shapes (non-spherical) with a mean particle size of less than 10 μm. W and WC present irregular polygonal particles with an average size of 1.5 μm.

Electrolytic Co exhibits irregular shapes and forms aggregates, as shown in Figures 4-B to 4-D. In contrast, Ni powder consists of dendritic and porous particles, each smaller than 10 μm. The fluidity of powders is not an inherent property, which depends not only on the physical properties but also on the state of stress, the equipment used, and the handling method. Powder flow in individual methods of AM is a complex area of study (Zegzulka *et al.*, 2020).

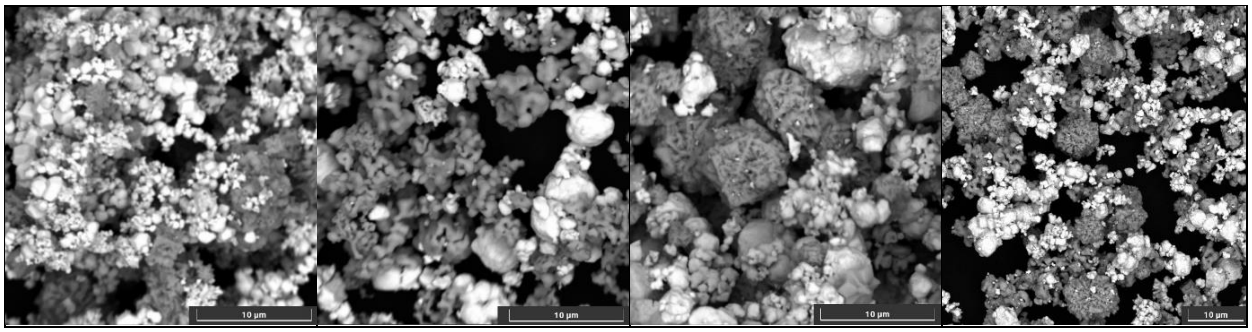

Figure 4 – MEV images of powder mixtures of alloys: (A) 70W-30Ni, (B) 70WC-30Co, (C) 70WC-30Ni, and (D).

The stability test (Figure 5) showed that all the mixtures are stable after 6 repetitions, and the BFE measured for each mixture is accurate. The mixture 70WC-30Co showed the lowest BFE, and incorporating Co in the sample containing only Ni reduces its basic flow energy, improving its flowability. Using Co alone proves to be more effective in reducing the flow energy of the WC powder. Thus, Co seems to act as an attenuator of interparticle interactions, allowing more effortless movement of powder bed particles. To eliminate the effect of the density of each type of material on the energy consumed by the blade when crossing the powder bed, BFE was divided by the mass of material that constitutes the powder bed used, resulting in the flow energy per gram of material moved: BFE/mass of material. The results are shown in Table IV.

Table IV – BFE and VFR results.

Sample	BFE (mJ)	Bulk Density ($g.cm^{-3}$)	Mass (g)	BFE/g (mJ/g)
70WC-30Co	4007.11	3.96	634.31	6.317
70WC-30Ni	3606.39	3.53	564.88	6.384
70WC-30(Co,Ni)	2623.04	3.17	507.74	5.166
70W-30Ni	2727.93	3.02	483.19	5.646

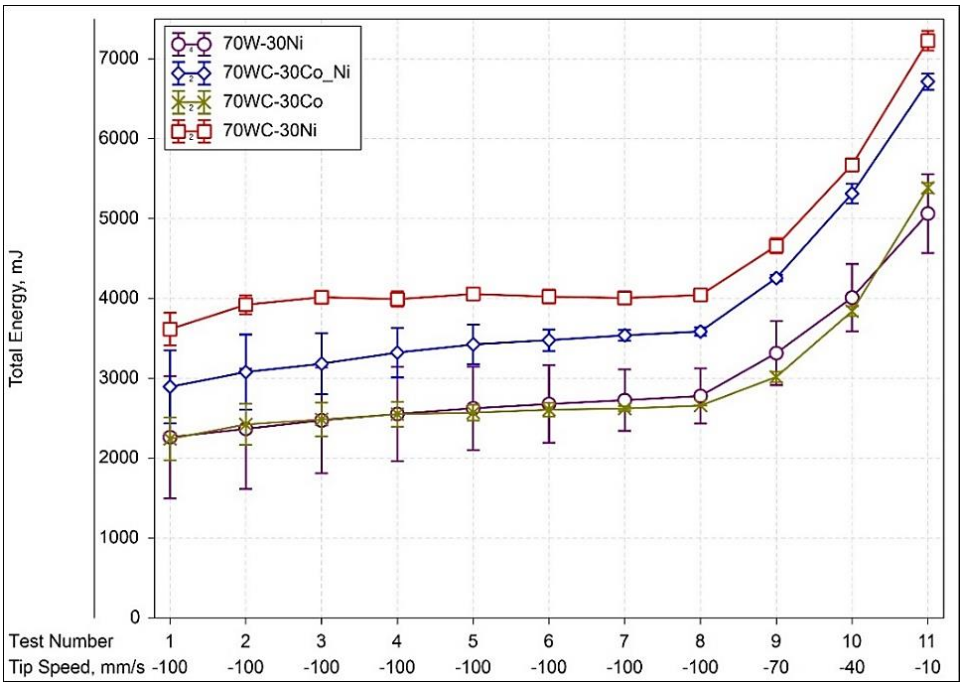

Figure 5 - Graphical results of the stability test (tests 1-7), the basic flow energy measurement - BFE (tests 6-7), and the variable flow energy -VFR (tests 8-11).

The effort per unit mass required to move the 70WC-30Co and 70W-30Ni samples appears nearly identical. Adding Co with Ni to form the WC-30(Co,Ni) powder mixture does not significantly improve BFE compared to the WC-Co powder mixture.

Surprisingly, the basic flow energy for the 70W-30Ni mixture was almost as low as that of 70WC-30Co and also presented a small value for BFE/mass, despite W being denser (19.23 $g.cm^{-3}$) than WC (15.64 $g.cm^{-3}$). It was expected that more energy would be necessary to move the denser W particles. However, the properties of the 70W-30Ni mixture are different from pure W powder, even though W is the significant component.

The same is observed for all other mixtures. It can be seen in Figure 6 that samples containing W are more compressible than the WC samples, regardless of the addition of different compounds. Thus, it is possible to state that the W sample has higher porosity, producing a bed of particles with more significant voids. This explains this sample's lowest expended energy and bulk density value.

Data obtained from the compressibility test of mixtures based on WC and W are presented in Table V. The 70WC-30Ni exhibits less compressible behavior, inferring its attempt at a better packaging condition, corroborating the highest level of basic flow energy investigated. Moreover, the 70WC-30Co mixture presented intermediate compressibility, similar to 70WC-30(Co,Ni), despite similar basic flow energy from 70W-30Ni, indicating that mechanical interlocks are a phenomenon to be considered in packing conditions of non-spherical samples.

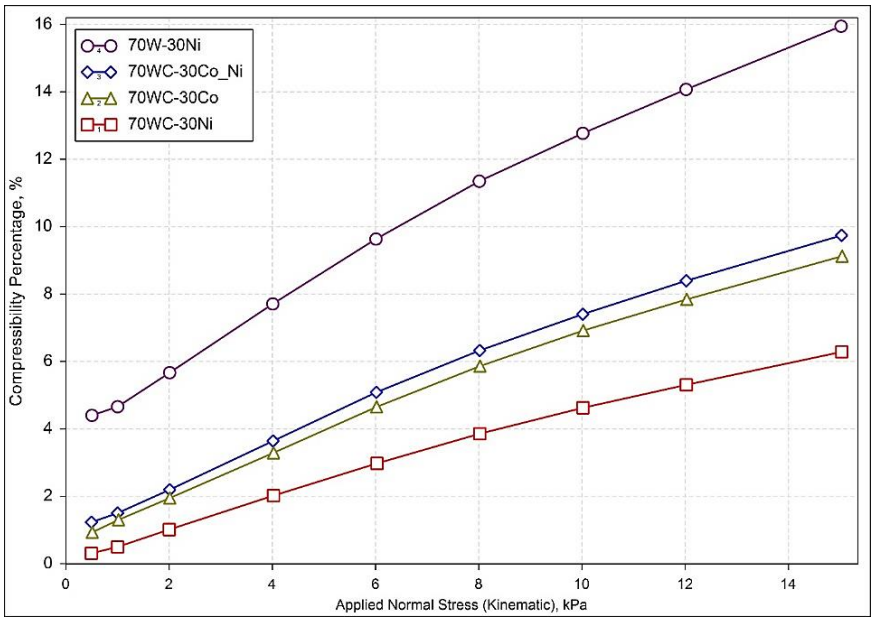

Figure 6 - Compressibility test of WC and W-based mixtures.

Table V – Relationship between bulk density and compressed density (BDcomp).

	Sample	Bulk Density (g/cm^3)	CPS (%) @ 15 kPa	Split Mass (g)	$BD_{comp.}$ (g/cm^3)
(I)	70WC-30Co	3.33	9.13	282.91	3.66
(II)	70WC-30Ni	4.11	6.29	349.42	4.39
(III)	70WC-30(Co,Ni)	3.60	9.74	306.01	3.99
(IV)	70W-30Ni	3.27	15.9	349.42	4.88

The aeration test is essentially the BFE test with air supplied at the base of the powder bed, in which the BFE is measured as a function of the amount of air injected into the system. The graphical results of the aeration test are presented in Figure 7.

Since part of the volume initially occupied by solids is now taken up by air, the blade will exert less force to pass through the particle bed. If the powder is non-cohesive, the air will permeate the bed easily, resulting in a significantly lower BFE compared to the original BFE (without air supply).

The results indicate complete fluidization of all samples at an air velocity of 15 mm/s, but a considerable reduction in BFE is yet noticed at low flow rates (2.5 to 5.0 mm/s).

It seems that the samples containing Ni and Co exhibit two stages of energy stabilization, possibly corresponding to two phases of fluidization: the first for smaller particles (fines) and the second for the larger particles. (Consider analyzing the particle size distribution to determine if it is bimodal).

An important observation is the behavior of the samples containing 70WC-30Ni, which shows that the mixture is more cohesive when compared to the mixture containing 70W-30Ni. The 70WC-30(Co, Ni) sample presents the highest cohesion compared to the 70WC-30Ni and 70WC-30Co mixtures. The shape and size of the Ni and Co particles were influenced significantly, indicating that the interactions between different components are essential in the fluidity of the studied samples.

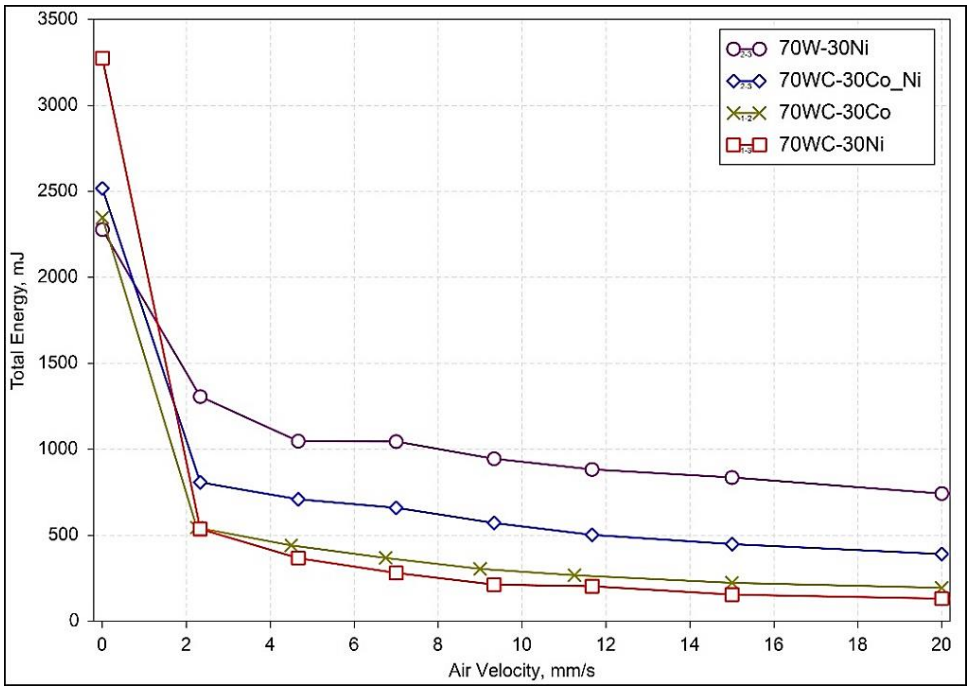

Figure 7 - Aeration test of WC and W-based mixtures.

To evaluate the frictional properties of the particles constituting the mixtures, shear tests were performed at 4 different consolidation states (3, 6, 9, and 15 kPa). Figures 8 to 11 show the shear results and indicate, once again, that the 70W-30Ni sample presents the most cohesive behavior. However, the incorporation of Cobalt in WC enhances its flow properties.

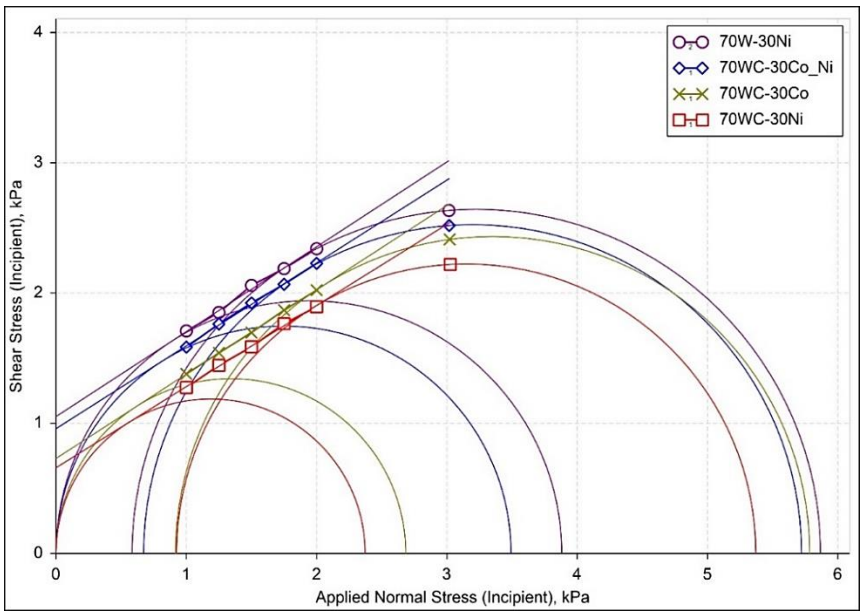

Figure 8 - Shear test for quantitative measurement of cohesion at 3 kPa.

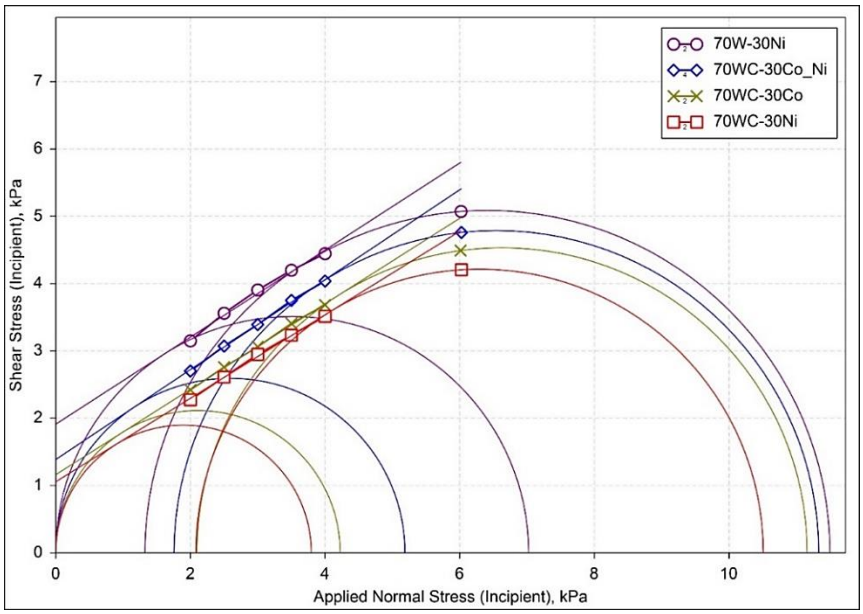

Figure 9 - Shear test for quantitative measurement of cohesion at 6 kPa.

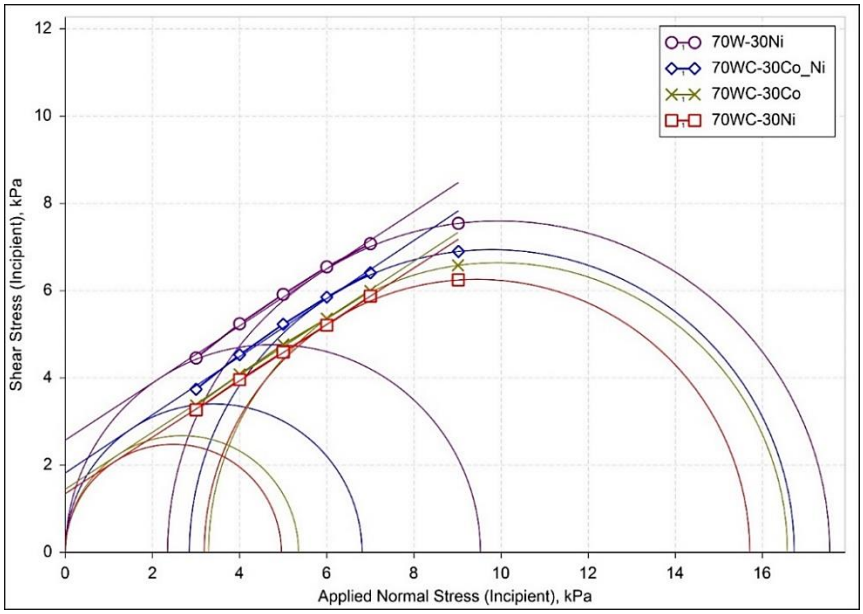

Figure 10 - Shear test for quantitative measurement of cohesion at 9 kPa.

The 70WC-30Ni sample demonstrates the most favorable flow characteristics among the samples containing only Co. Reliable flow of cohesive powders is a significant challenge to achieve in various particle processing operations, such as silo and hopper unloading, feeding, dosing, etc., where shear strength is assessed under specific consolidation stress or packing conditions. Typically, this evaluation involves moderate to high stresses and very low shear strain rates (Costa, Costa & Condotta, 2015; *Hare et al.*, 2015).

In Additive Manufacturing via L-PBF, this dry powder deposition technique shows promise, offering the advantage of being applicable with small quantities of WC and W-based powder composites in the vibrating device. However, further investigation into its behavior in the dynamic regime is needed, with increased measurement repetitions, to more effectively differentiate between powders with similar rheological properties across all packing states.

This type of dry granulation is neither suitable nor commonly used for processing via L-PBF techniques. It is more frequently applied in conventional liquid-phase sintering. The literature does

not provide information on which formulation properties are suitable or unsuitable for this processing method.

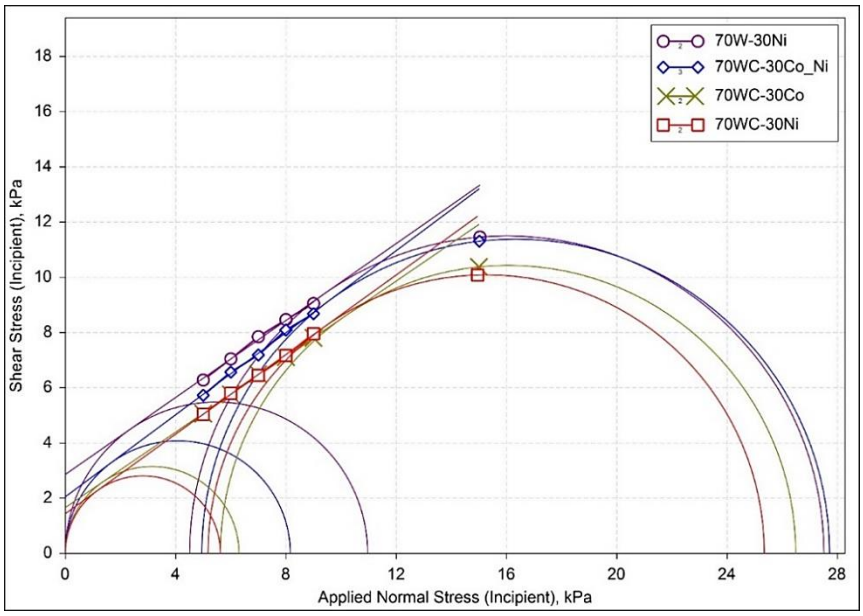

Figure 11 - Shear test for quantitative measurement of cohesion at 15 kPa.

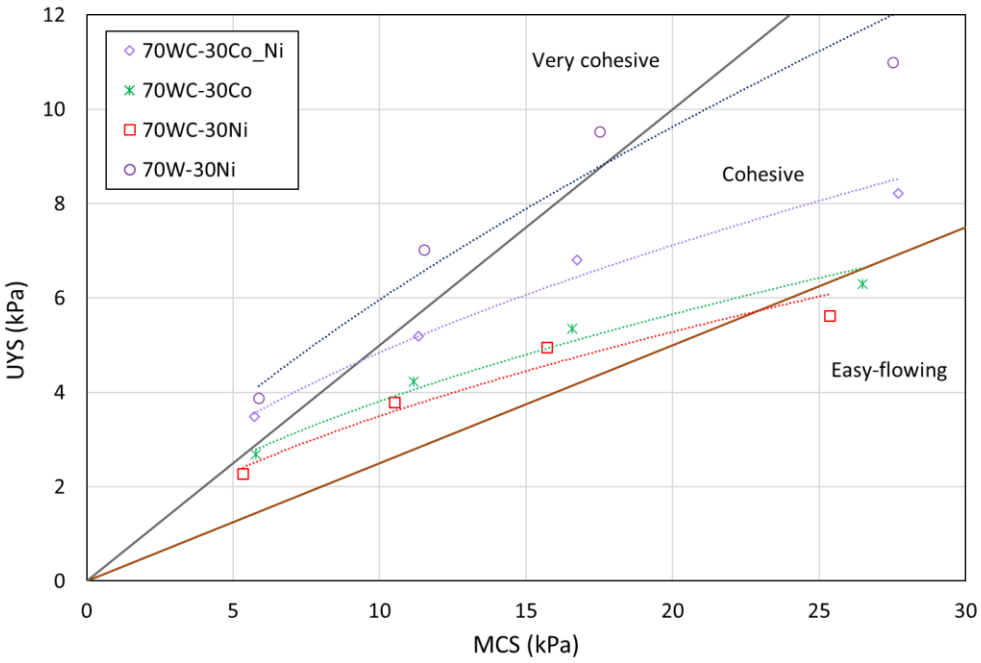

Figure 12 - Classification of the flow profile of the studied mixtures.

Finally, shear tests also provide the flow function of materials, which classifies their flow profile, presented in Figure 12. Observing the cohesion values of the samples, it is concluded the 70WC-30Ni sample is the most cohesive, corroborating the aeration test results and the basic flow energy per unit mass (BFE/g) obtained, while the 70WC-30Ni and 70W-30Co samples had the lowest cohesion values and better flow pattern.

4. Conclusions

This work allowed us to arrive at the following considerations:

I. The best flow conditions are observed in samples of 70WC-30Ni and 70WC-30(Co,Ni), which have good fluidity, but samples of 70WC-30Co and 70W-30Ni have poor fluidity;

II. Adding Co with WC and WC-Ni improves the Basic Flow Energy (BFE). Only Ni with WC worsens the BFE;

III. The 70WC-30Ni mixture showed lower porosity and the 70W-30Ni mixture the highest, requiring a better compaction technique in the powder bed to produce a flawless part;

IV. The packing of the 70W-30Ni mixture indicates a higher cohesiveness of this mixture compared to the WC-based alloys due to the increase in particle size and/or density; and

V. When mixed with W and WC refractories, the particle size of nickel tends to flow more freely in the powder bed, allowing the particles to slide over each other and form a more compacted bed.

Acknowledgements

The authors would like to thank the company Brats Indústria e Comércio de Produtos Metálicos Especiais Ltda for the partnership and the Centro Universitário da FEI for the support and use of the FT- 4 Powder Rheometer® and the Fundação de Amparo à Pesquisa do Estado de São Paulo (FAPESP), Brazil, for the financial support; Grant number: 2022/06201-7.

References

Budding, A., Vaneker, T. (2013) New Strategies for Powder Compaction in Powder-based Rapid Prototyping Techniques. *Procedia CIRP*. 6. 528–533. https://doi.org/10.1016/j.procir.2013.03.100

Costa, E. B., Costa, R. A., Condotta, R. (2015) Flowability of halogen-free flame retardant polymeric compositions. *Chemical Engineering Transactions*, 43. doi: https://doi.org/10.3303/CET1543135

Debroy, T., Wei, H., Zuback, J., Mukherjee, T., Elmer, J., Milewski, J.O., Beese, A., Wilson-Heid, A., De, A., Zhang, W. (2018). Additive manufacturing of metallic components - Process, structure, and properties. *Progress in Materials Science*, 92, 112-224. https://doi.org/10.1016/j.pmatsci.2017.10.001

Freeman, T., Bey, H., Hanish, M., Brockbank, K., Armstrong, B. (2016). The influence of roller compaction processing variables on the rheological properties of granules. *Asian Journal of Pharmaceutical Sciences*. 11. 516-527. https://doi.org/10.1016/j.ajps.2016.03.002

Freeman, R. (2007) Measuring the flow properties of consolidated, conditioned and aerated powders — A comparative study using a powder rheometer and a rotational shear cell, Powder Technology, 174(1-2), 25-33. https://doi.org/10.1016/j.powtec.2006.10.016

Gururajan, B.; Seville, J.P.K.; Adams, M.; Greenwood, R.; Fitzpatrick, S. (2005). Roll compaction of a pharmaceutical excipient: Experimental validation of rolling theory for granular solids. *Chemical Engineering Science*, 60. 3891-3897. https://doi.org/10.1016/j.ces.2005.02.022

Hare, C., Zafar, U., Ghadiri, M., Freeman, T., Clayton, J., Murtagh, M. (2015). Analysis of the dynamics of the FT4 powder rheometer. *Powder Technology*, 285, 123-127. https://doi.org/10.1016/j.powtec.2015.04.039

Marchetti, L., Hulme-Smith, C. (2021). Flowability of steel and tool steel powders: A comparison between testing methods. *Powder Technology*, 384. 402-413.https://doi.org/10.1016/j.powtec.2021.01.074

Miranda, F., Maiolini, A., dos Santos, M. O., Rodrigues, D., Janasi, S. R., Batalha, G. F. (2023a) Towards the flowability and spreadability of cemented carbides and cermet powders for

Additive Manufacturing: experimental and numerical approach - Part 1. *27th International Congress of Mechanical Engineering*. Rio de Janeiro, Brazil. https://doi.org/10.26678/ABCM.COBEM2023.COB2023-0100

Miranda, F., dos Santos, M. O., Rodrigues, D., Coelho R. S., Batalha, G. F. (2023b) NbC-based cermet production comparison: L-PBF additive manufacturing versus conventional LPS powder metallurgy. *MatTech*, 57 (5), 465–473. doi: https://doi.org/10.17222/mit.2023.972

Miranda, F., dos Santos, M. O., Condotta, R., Pereira, N. M. G., Rodrigues, D., Janasi, S. R., Ortega, F. d. S., Mergulhão, M. V., Coelho, R. S., de Oliveira, R. R., Martinez, L. G., & Batalha, G. F. (2024). Additive Manufacturing of Tungsten Carbide (WC)-Based Cemented Carbides and Niobium Carbide (NbC)-Based Cermets with High Binder Content via Laser Powder Bed Fusion. Metals, 14(12), 1333. https://doi.org/10.3390/met14121333

Pal, S., Drstvensek, I., Brajlih, T. (2018) Physical behaviors of materials in selective laser melting process. DAAAM International Scientific Book. https://doi.org/10.2507/daaam.scibook.2018.21

Zegzulka, J., Gelnar, D., Jezerská, L., Prokes, R., Rozbroj, J. (2020). Characterization and flowability methods for metal powders. *Scientific Reports.* 10. https://doi.org/10.1038/s41598-020-77974-3